Proceedings of the ASME 2020 Fluids Engineering Division Summer Meeting
FEDSM2020
July 13-15, 2020, Virtual, Online

FEDSM2020-20073

MICRO MACHINED SLIT BETWEEN RIDGE AND GROOVE IN MICRO FLUID-CHANNEL TO MEASURE FLOATING CELL DEFORMABILITY

Shigehiro Hashimoto[1]
Kogakuin University,
Tokyo, 1638677, Japan

ABSTRACT

A micro-slit has been designed to measure deformation of a biological single cell passing through the slit. At the middle part of the flow channel, the slit (7 μm height, 0.4 mm width, and 0.1 mm length) has been made by photolithography technique: the combination of the micro-ridge on the transparent polydimethylsiloxane plate and the micro-groove on the glass plate. C2C12 (mouse myoblast cells) was used in the test. The flow of suspension of cells was controlled by the pressure head between the inlet and the outlet. Deformation of cells passing through the micro slit was observed with an inverted phase-contrast microscope. The experimental results show that a cell deforms to the flat circular disk and passes through the micro-slit. Although smaller cells tend to pass the micro-slit easily, some bigger cells also passed the micro-slit. Deformation ratio is independent of the size of each cell. The designed slit has capability to detect quantitative deformability of a single biological cell.

Keywords: Biomedical Engineering, Photolithography, Micro-slit and C2C12

NOMENCLATURE

D	diameter of cell
h	height of slit
l	length of slit
Re	Reynolds number
Rx	increase rate of projected length per time
S_1	area of cell before slit
S_2	area of cell in slit
S_3	area of cell after slit
S_i	calculated area of cell in slit
t	time
v	velocity of flow before the slit
w	width of slit
x	projected length
η	viscosity of fluid
ρ	density of fluid

1. INTRODUCTION

Deformability of each biological cell plays an important role in bio-microfluidics *in vivo*. An erythrocyte, for example, has high flexibility, and deforms in the shear flow [1]. The deformed cell also passes through the capillary in the micro-circulation, of which the dimension is smaller than the diameter of the biconcave disc shape of erythrocyte [2]. After circulation through the blood vessels for days, the erythrocyte is trapped in the micro-circulation systems [3].

A slit is one of the systems, which sorts biological cells *in vivo*. Sorting at the slit depends not only on the size of each cell, but also on the deformability of each cell [4]. Several cells are able to pass through very narrow slits: cancer cells [5], or white blood cells. The slit may play important role to distinguish several properties of each cell: cell types, defects of membrane, and viability. The recently developed photolithography technique [6] enables manufacturing the micro-topography in the flow channel [7]. Behavior of cells in the flow channel [8] will be applied to cell sorting [9]. The photolithography technique can be applied to make a micro-slit [10]. The slit between micro cylinders was made to sort cells in the previous study [11]. The deformation of the depth direction between cylinders, however, cannot be observed by the conventional optical microscope.

To observe the deformed cell at the direction perpendicular to the walls of the slit, another type of the slit is designed with the combination of the micro-ridge and the micro-groove in the present study. In the present study, a micro-slit has been fabricated in a flow channel by the photolithography technique, and deformation of a biological cell passing through the micro slit has been observed *in vitro*.

[1] Contact author: shashimoto@cc.kogakuin.ac.jp

2. MATERIALS AND METHODS

2.1 Micro-slit

The slit has been designed between the transparent polydimethylsiloxane (PDMS) plate and the borosilicate glass (Tempax) plate (Fig. 1). The dimension of the slit is as follows: the width (*w*) of 0.4 mm, the length (*l*) of 0.1 mm, and the height (*h*) of 7 μm. The upper plate of PDMS has the rectangular groove: the depth (*d*) of 0.03 mm, the width of 0.6 mm, and the length of 16 mm (separated into two half parts with the interval of 0.1 mm length (*l*)). The lower plate of the glass has the rectangular groove: the depth (*h*) of 7 μm, the width (*w*) of 0.4 mm, and the length of 1 mm. These plates keep contact to make slits between them. The slit is located at the middle part of the flow channel.

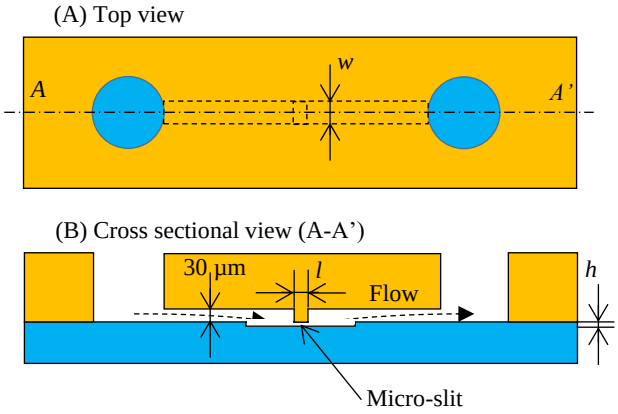

FIGURE 1: MICRO SLIT IN FLOW CHANNEL

2.2 Photomask for Upper Plate

A glass plate (36 mm × 26 mm × 1 mm: Matsunami Glass Ind., Ltd., Osaka, Japan) was used for the base of the photomask (A) (Fig. 2). The glass plate was cleaned by an ultrasonic cleaner with the alkaline solution, and rinsed by the ultrapure water. After the alkaline cleaning, the surface of the glass plate was exposed to oxygen (100 cm^3/min, 1013 hPa) plasma ashing for ten minutes at 200 W at 20 Pa by RIE-10NR (Samco International, Kyoto, Japan). Titanium was coated on the surface with 0.15 μm thick in the electron beam vapor deposition apparatus (JBS-Z0501EVC, JEOL Ltd., Japan) at the deposition rate of 0.1 nm/s (the back pressure of 8.0×10^{-4} Pa) (Fig 2-1).

The surface of the glass plate was hydrophilized by oxygen (100 cm^3/min, 1013 hPa) plasma ashing for ten minutes at 200 W at 20 Pa by RIE-10NR. The positive photoresist material of OFPR-800LB (Tokyo Ohka Kogyo Co., Ltd, Tokyo, Japan) was coated on the titanium layer at the disk at 3000 rpm for 30 s with the spin coater (1H-DX2, Mikasa Co. Ltd., Tokyo, Japan) (Fig. 2-2). The photoresist was baked on the heated plate at 368 K for one minute.

The pattern was drawn on the photomask with the laser drawing system (DDB-201K-KH, Neoark Corporation, Hachioji, Japan) (Fig. 2-3). To control the dimension of the pattern on the photomask with the laser drawing system, the parameters were selected as follows: the voltage of 3.25 V, the velocity of 0.17 mm/s, the acceleration of 0.37 mm/s^2, and the focus offset at +4.0.

The photoresist was developed with tetra-methyl-ammonium hydroxide (NMD-3, Tokyo Ohka Kogyo Co., Ltd., Kawasaki, Japan) for 3 minutes (Fig. 2-4). The disk was rinsed by the ultrapure water, and dried by the spin-dryer (with N_2 gas at 1100 min^{-1} for 30 seconds).

The titanium coated disk was etched with the plasma gas using RIE-10NR (Samco International, Kyoto, Japan) (Fig. 2-5). For etching, the gas of SF_6 (50 cm^3/min at 1013 hPa) with Ar (50 cm^3/min at 1013 hPa) was applied at 75 W at 4 Pa for ten minutes.

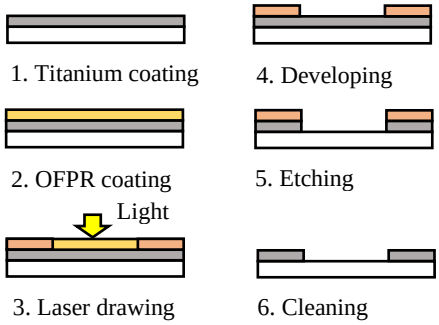

FIGURE 2: PHOTOLITHOGRAPHY PROCESS OF PHOTOMASK (A) FOR UPPER PLATE

2.3 Mold for Upper Plate

A glass plate (36 mm × 26 mm × 1 mm) was used for the surface mold for the upper disk (Fig. 3). The plate was cleaned by an ultrasonic cleaner with alkaline solution for ten minutes, and rinsed by the ultrapure water for ten minutes. The surface of the glass plate was hydrophilized by oxygen (30 cm^3/min, 0.1 Pa) plasma ashing for ten minutes at 200 W by the reactive ion etching system (FA-1). The negative photoresist material of high viscosity (SU8-10: Micro Chem Corp., MA, USA) was coated on the glass plate at 1000 rpm for 30 s with a spin coater (Fig. 3-1). After the photoresist was baked on the heated plate at 338 K for five minutes, the plate was baked on the heated plate at 368 K for ten minutes.

The photomask (A) was mounted on the surface of SU8-10, and the photoresist was exposed to the ultraviolet (UV) light through the photomask in the mask aligner (M-1S, Mikasa Co. Ltd., Japan) at 15.85 mW/cm^2 for 20 s (Fig. 3-2). After the photoresist was baked on the heated plate at 338 K for one minute, the plate was baked on the heated plate at 368 K for five minutes.

The photoresist was developed with SU-8 developer (Nippon Kayaku Co., Ltd, Tokyo, Japan) for ten minutes (Fig. 3-3). The glass surface with the micro pattern was rinsed with IPA (2-propanol, Wako Pure Chemical Industries, Ltd.) for five minutes, and with the ultrapure water. The plate was dried by the spin-dryer. The photoresist was baked on the heated plate at 368 K for three minutes.

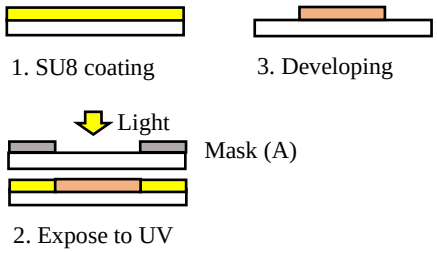

FIGURE 3: PHOTOLITHOGRAPHY PROCESS OF MOLD FOR UPPER PLATE

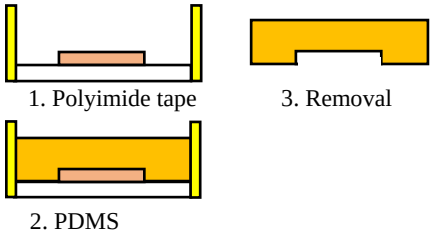

FIGURE 4: MACHINING PROCESS OF UPPER PLATE

2.4 Upper Plate

After the mold of the glass plate was enclosed with the peripheral wall of polyimide (Fig. 4-1), PDMS (Sylgard 184 Silicone Elastomer Base, Dow Corning Corporation) was poured together with the curing agent (Dow Corning Corporation) on the mold (Fig. 4-2). The volume ratio of curing agent is ten percent of PDMS. After degassing, PDMS was baked at 373 K for one hour in the oven (DX401, Yamato Scientific Co., Ltd, Tokyo, Japan). The baked plate of PDMS is exfoliated from the mold (Fig. 4-3). Two holes of 3 mm diameter were machined with a punching tool at the upper disk to make the inlet and the outlet for the flow channel.

2.5 Photomask for Lower Plate

A glass plate (36 mm × 26 mm × 1 mm) was used for the base of the photomask (B) (ref. Fig. 2). The glass plate was cleaned by the ultrasonic cleaner with the alkaline solution, and rinsed by the ultrapure water. After the alkaline cleaning, the surface of the glass plate was exposed to oxygen (30 cm^3/min, 1013 hPa) plasma ashing for ten minutes at 200 W at 20 Pa by RIE-10NR. Titanium was coated on the surface with 0.15 µm thick in the electron beam vapor deposition apparatus (JBS-Z0501EVC) at the deposition rate of 0.1 nm/s (the back pressure of 8.0×10^{-4} Pa).

The surface of the glass plate was hydrophilized by oxygen (100 cm^3/min, 1013 hPa) plasma ashing for ten minutes at 200 W at 20 Pa by RIE-10NR. The positive photoresist material of OFPR-800LB was coated on the titanium layer at the disk at 3000 rpm for 30 s with the spin coater. The photoresist was baked on the heated plate at 368 K for one minute.

The pattern was drawn on the photomask with the laser drawing system (DDB-201K-KH). To control the dimension of the pattern on the photomask with the laser drawing system, the parameters were selected as follows: the voltage of 3.25 V, the velocity of 0.17 mm/s, the acceleration of 0.37 mm/s^2, and the focus offset at +4.0.

The photoresist was developed with tetra-methyl-ammonium hydroxide (NMD-3, Tokyo Ohka Kogyo Co., Ltd., Kawasaki, Japan) for 3 minutes. The disk was rinsed by the ultrapure water, and dried by the spin-dryer. The titanium coating disk was etched with the plasma gas (SF_6, Ar) using RIE-10NR. For etching, the gas of SF_6 (50 cm^3/min at 1013 hPa) with Ar (50 cm^3/min at 1013 hPa) was applied at 75 W at 4 Pa for ten minutes.

A glass plate (36 mm × 26 mm × 1 mm) was used for the base of the photomask (C). After the alkaline cleaning, the surface of the glass plate was exposed to oxygen (100 cm^3/min, 1013 hPa) plasma ashing for ten minutes at 200 W at 20 Pa by RIE-10NR. Titanium was coated on the surface with 0.15 µm thick in the electron beam vapor deposition apparatus (JBS-Z0501EVC) at the deposition rate of 0.1 nm/s (the back pressure of 8.0×10^{-4} Pa). The surface of the glass plate was hydrophilized by oxygen (100 cm^3/min, 1013 hPa) plasma ashing for ten minutes at 200 W at 20 Pa by RIE-10NR. The negative photoresist material (SU8-2: Micro Chem Corp.) was coated on the glass plate at 2000 rpm for 30 s with the spin coater. After the photoresist was baked on the heated plate at 338 K for one minute, the plate was baked on the heated plate at 368 K for one minute.

The photomask (B) was mounted on the surface of SU8-2, and the photoresist was exposed to the UV light through the mask in the mask aligner (M-1S) at 15.85 mW/cm^2 for 8 s (ref. Fig. 3-2). After the photoresist was baked on the heated plate at 338 K for one minute, the plate was baked on the heated plate at 368 K for three minutes. The photoresist was developed with SU-8 developer for five minutes. The disk was rinsed by the ultrapure water, and dried by the spin-dryer (with N_2 gas at 1100 min^{-1} for 30 seconds). The titanium coated disk was etched with the plasma gas (SF_6, Ar) using RIE-10NR. For etching, the gas of SF_6 (50 cm^3/min at 1013 hPa) with Ar (50 cm^3/min at 1013 hPa) was applied at 75 W at 4 Pa for ten minutes.

2.6 Lower Plate

A glass plate (36 mm × 26 mm × 1 mm) was used for the surface for the upper disk. The plate was cleaned by the ultrasonic cleaner with alkaline solution for ten minutes, and rinsed by the ultrapure water for ten minutes. The surface of the glass plate was hydrophilized by oxygen (30 cm^3/min, 0.1 Pa) plasma ashing for ten minutes at 200 W by the reactive ion etching system (FA-1). The negative photoresist material of high viscosity (SU8-5) was coated on the glass plate at 1400 rpm for 30 s with the spin coater. After the photoresist was baked on the heated plate at 338 K for two minutes, the plate was baked on the heated plate at 368 K for five minutes. The photomask (C) was mounted on the surface of SU8-5, and the photoresist was exposed to the UV light through the photomask in the mask aligner (M-1S) at 15.85 mW/cm^2 for 20 s (ref. Fig. 3-2). After the photoresist was baked on the heated plate at 338 K for one minute, the plate was baked on the heated plate at 368 K for two

minutes. The photoresist was developed with SU-8 developer for two minutes. The dimension of the depth of the groove was measured by the stylus of the contact profilometer (Dektak XT-E, Bruker Corporation).

2.7 Flow Channel

The lower plate with the micro pattern was rinsed with IPA (2-propanol), and with the ultrapure water. The plate was dried by the spin-dryer. The surface of the plate was exposed to oxygen (100 cm^3/min, 1013 hPa) plasma ashing for one minute at 40 W at 20 Pa by RIE-10NR. The plate was rinsed with aminopropyltriethoxysilane (APTES) for ten minutes, and with the ultrapure water. After the plate was dried, the upper plate was adhered on the lower plate. The plates were baked in the oven at 368 K for ten minutes.

2.8 Flow Test

C2C12 (mouse myoblast cell line originated with cross-striated muscle of C3H mouse) was used in the flow test. D-MEM (Dulbecco's Modified Eagle Medium) was used for the medium. Each medium contains 10% FBS (decomplemented fetal bovine serum) and 1% penicillin/ streptomycin (GIBCO, Life Technologies Japan Ltd., Tokyo, Japan).

The cells were exfoliated from the bottom of the culture dish with trypsin, and suspended in the culture medium (1000 cells/cm^3). Before the flow test, the flow channel was hydrophilized by oxygen (100 cm^3/min, 1013 hPa) plasma ashing for one minute at 40 W at 20 Pa by RIE-10NR. The bovine serum albumin solution was prefilled in the flow channel, and incubated for ten minutes at 310 K in the incubator.

The suspension of the cells was poured at the inlet of the flow channel. The suspension flows by the pressure head of 2.5 mm, which makes the pressure difference of 25 Pa between the inlet and the outlet. The flow rate decreases gradually with the decrease of the pressure head. The behavior of cells near the slit was observed with the inverted phase-contrast microscope (IX71, Olympus Co., Ltd., Tokyo) (Fig. 5).

2.9 Image Analysis

The microscopic images of thirty frames per second at the shutter speed of 1/2000 s were captured by the camera (DSC-RX100M4, Sony Corporation, Tokyo, Japan) (Fig. 5). At the images, the contour of each cell was traced with "Image J", and the projected area (S) was calculated. A cell stops at the wall of the slit before entry of the slit. Assuming spherical shape before entry of the slit, the equivalent diameter (D) of each floating cell is calculated by Eq. (1).

$$D = 2\,(S / \pi)^{1/2} \tag{1}$$

The areas of cells were calculated: before the slit (S_1), in the slit (S_2), and after the slit (S_3) (Fig. 6). Assuming the deformation of each cell from the sphere to cylindrical plate as the first approximation, the equivalent projected area in the slit (Si) was calculated by Eq. (2).

$$Si = (4\,S_1^{1.5}) / (3\,h\,\pi^{0.5}) \tag{2}$$

In Eq. (2), h is the height of the slit. Some cells deform partially to project the part of the body into the slit at the edge of the entry of the slit (Fig. 5a). The projected length (x) (Fig. 6) at the direction of downstream in the slit was measured. The deformation was traced for three minutes, and the increase rate (Rx) of x per time (t) was calculated at each cell by Eq. (3).

$$Rx = \Delta x / \Delta t \tag{3}$$

3. RESULTS

The measurement by the stylus of the contact profilometer shows that the depth of the groove on the lower plate is 7.3 μm, which corresponds to the height (h) of the slit.

The small flowing particle shows that the mean flow velocity (v) in the cross section of the flow channel before the slit is in the range between 2 mm/s and 10 mm/s. In the slit, the mean medium velocity is eight times higher than that of before the slit because of the cross-sectional area change.

Every cell stopped at the entry edge of the slit, before got into the slit (Fig. 5a). Some cells passed through the slit (Fig. 5b). Every cell kept approximately circle shape at the contour of the projected area during passing through the slit (Fig. 5b). Every cell maintained the constant project area during passing through the slit. The results of the test at nineteen cells were divided into three groups: A, B, and C. Eight cells were captured at the entry edge of the slit (A). Six cells were staying in the slit (B). Five cells passed through the slit (C). In each group, the mean values of S (projected area before the slit) were 306±65 μm^2 (A), 248±50 μm^2 (B), and 232±23 μm^2 (C), respectively. The equivalent diameter (D) of the cell calculated by the mean value of S were 20 μm (A), 18 μm (B), and 17 μm (C), respectively.

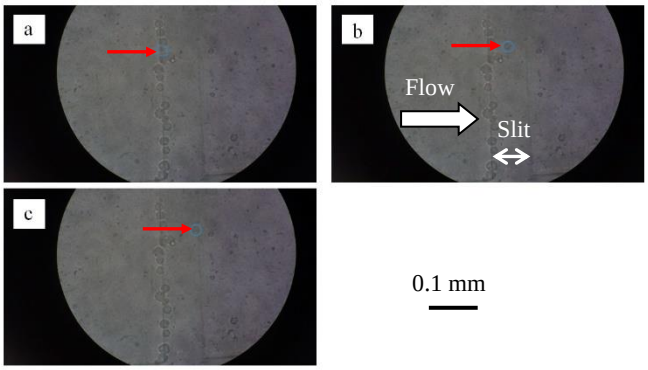

FIGURE 5: C2C12 (RED ARROW) MOVEMENT AT SLIT: ENTER TO SLIT (a), PASSING THROUGH SLIT (b), GET OUT OF SLIT (c)

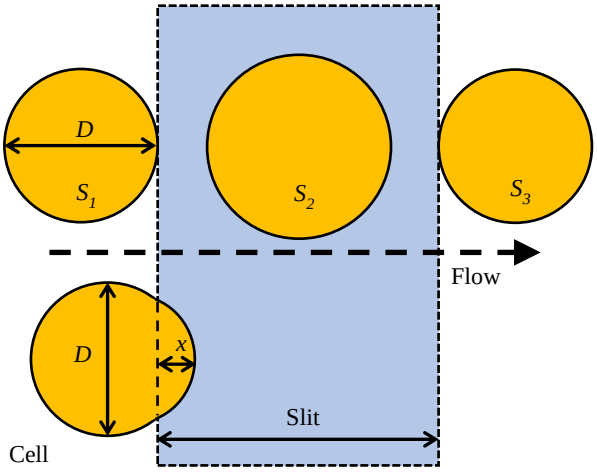

FIGURE 6: MEASUREMENT OF CELL AT SLIT

Fig. 7 shows the projected area of each cell before the slit (S_1) and in the slit (S_2) in the group B. The projected area (S) increases in every cell (solid line). The dotted line shows the increase to the calculated value of Si. The rate of increase does not depend on the size of the cell. Each projected area (S) of some bigger cells does not increase as much as the calculated value (Si), respectively. Fig. 8 shows the projected area history (before the slit (S_1), in the slit (S_2), and after the slit (S_3)) of each cell passing through the slit in the group C. The dotted line shows the increase to Si calculated by Eq. (3). Si is connected by dotted line, which starts from S_1 and returns to S_1 through Si in Fig. 8. In every cell, each projected area increases from S_1 to S_2 to pass the slit. In every cell, the projected area (S) of the cell do not increase as much as calculated value (Si). One bigger cell passes the slit with small deformation (with the straight line in Fig. 8). The projected area of one cell does not return to original value after passing of the slit.

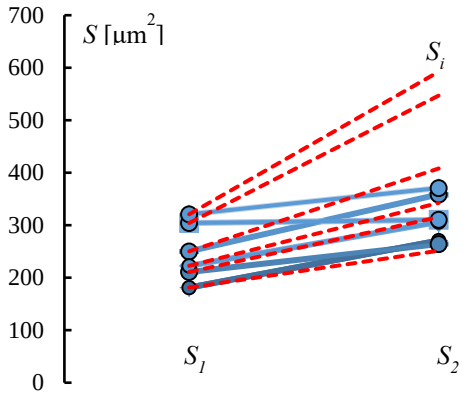

FIGURE 7: S BEFORE SLIT (S_1: LEFT), IN SLIT (S_2: RIGHT), AND CALCULATED Si IN SLIT CONNECTED BY DOTTED LINE

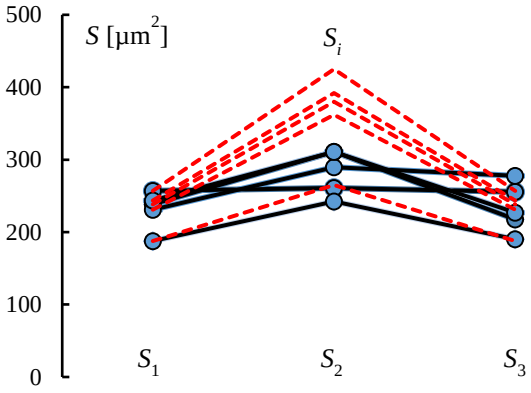

FIGURE 8: S BEFORE SLIT (S_1: LEFT), IN SLIT (S_2: MIDDLE), AND AFTER SLIT (S_3: RIGHT); DOTTED LINE STARTS FROM S_1 AND RETURNS TO S_1 THROUGH Si

Fig. 9 shows the partially projected length (x) of the cell body in relation to the equivalent diameter (D) of each cell before the entry of the slit. The equivalent diameter (D) of every cell is much bigger than the height of the slit (7.3 μm). Some bigger cell deforms to project the part of the cell body. Fig. 10 shows the increase rate (Rx) of the projected length of the cell body in relation to the equivalent diameter (D) of each cell before the entry of the slit. In some cells, the increase rate (Rx) of the partial projected length of the cell body is high regardless of the the equivalent diameter (D) of the cell.

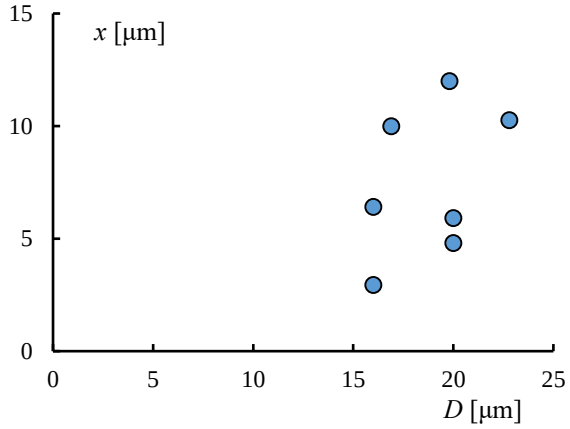

FIGURE 9: PROJECTED LENGTH (x) [μm] VS. EQUIVALENT DIAMETER (D) [μm] OF CELL

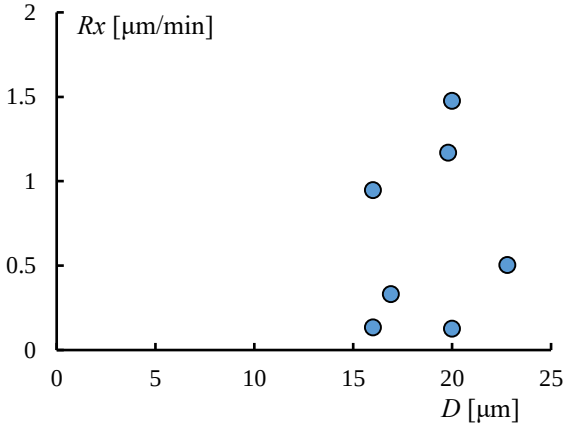

FIGURE 10: PROJECTED LENGTH INCREASE RATE (*Rx*) [μm/min] VS. EQUIVALENT DIAMETER (*D*) [μm] OF CELL

4. DISCUSSION

Deformation of a cell through a narrow slit was simulated in the previous study [4]. In the present study, the length of the slit is 0.l mm. The length of 0.1 mm is too long to simulate the slit *in vivo*. It is not easy, on the other hand, to manufacture the rigid narrow slit *in vitro* by micromachining. The wall of the slit should have enough strength to keep the precise topography against the fluid pressure to analyze the deformation of each cell *in vitro*. The glass surface is better than PDMS surface.

In Figs. 7 and 8, the projected area of each cell before the slit (S_1) exceeds 180 μm^2, so that the equivalent diameter (D) is bigger than 15 μm. The height of the slit is small enough to make deformation of each cell, which is passing through the slit.

Deformation, which is independent of the size of the cell, can be measured by the slit in the present study. The slit of the present study can distinguish cells by deformability. Deformability might depend on the contents of the cell. A ghost (vacant) cell might be more deformable than a normal cell. The recovery of the shape of the cell depends on elastic property of the cell (Fig. 8) [12]. The cell, which cannot recover to the original projected area, might have poor elasticity (Fig. 8).

The ridge of the PDMS has elasticity, so that the micro ridge may deform with the small ratio. The cell of the larger diameter is forced to be deformed at the higher deformation ratio in the slit. The higher deformation ratio makes the larger projected area in the slit. The higher deformation ratio would increase the frictional resistance at the slit. Several cells, which have the higher ratio between Si and S_2, may not be able to make enough deformation to pass through the slit (Fig. 7). Several cells, which cannot pass through the slit even with enough deformation ($S_2 = Si$), might show the high friction between the membrane and the wall of the slit (Fig. 7). The phenomena may relate to the deviated deformation of the cell.

The frictional resistance depends on the surface roughness, the surface waviness, and the surface adhesiveness. The dipping to the bovine serum albumin solution is effective to keep the property of the surface of the flow channel stable. Every cell kept the circle shape at the contour of the projected area during passing through the slit in the present study, which shows the flatness of the wall surface of the slit. Without prefill of the bovine serum albumin solution in the flow channel, most of cells adhere to the surface of the flow channel and hardly pass through the micro-slit in the present experiment.

The fine architecture of the red pulp of the spleen was investigated in the previous study [13]. In the previous studies, the typical micro channel had cylindrical shape with 5 μm diameter, which simulated the blood vessel capillary. The erythrocyte, on the other hand, passes through the micro slit narrower than 1 μm in the spleen. The deformability of erythrocyte changes with aging [14].

The deformation is evaluated with the change of the projected area of the disk during the passing through the slit in the present study. The deformation in the perpendicular direction can be observed with slit between weir-walls [15]. The difference between S_2 and Si relates to the convex peripheral part of the deformed disk of the cell. In some cases, the deformation takes time. During deformation, the volume of the cell can change by the penetration of liquid through the membrane.

The turbulent flow can make the irregular deformation on the cell. Reynolds number (Re) is calculated by Eq. (4).

$$Re = \rho\, v\, w/\, \eta \tag{4}$$

In Eq. (4), ρ is the density of the fluid, v is the velocity of the flow before the slit, w is the width of the channel before the slit, and η is the viscosity of the fluid. Re is 3, when ρ, v, w, and η are 10^3 kg m^{-3}, 10×10^{-3} m/s, 6×10^{-4} m, and 2×10^{-3} Pa s, respectively. The turbulent flow does not occur around the cell of this level of small value of Reynolds number.

5. CONCLUSION

The deformability of the single biological cell independent of its size can be detected by the micro-slit fabricated in the flow channel by the photolithography technique.

ACKNOWLEDGEMENTS

The author thanks to Dr. Yusuke Takahashi and Mr. Yuki Takiguchi for their assistance of the experiment.

REFERENCES

[1] Hashimoto, S., 2014, "Detect of Sublethal Damage with Cyclic Deformation of Erythrocyte in Shear Flow," Journal of Systemics Cybernetics and Informatics, 12(3), pp. 41-46.

[2] Skalak, R., and Branemark, P. I., 1969, "Deformation of Red Blood Cells in Capillaries," Science, 164(3880), pp. 717-719.

[3] Chen, L.T., and Weiss, L., 1973, "The Role of the Sinus Wall in the Passage of Erythrocytes through the Spleen," Blood, 41(4), pp. 529-537.

[4] Salehyara, S., and Zhu, Q., 2016, "Deformation and Internal Stress in a Red Blood Cell as It Is Driven through

a Slit by an Incoming Flow," Soft Matter, 12(13), pp. 3156-3164.

[5] Hou, H.W., Li, Q.S., Lee, G.Y.H., Kumar, A.P., Ong, C.N., and Lim, C.T., 2009, "Deformability Study of Breast Cancer Cells Using Microfluidics," Biomedical Microdevices, 11(3), pp. 557-564.

[6] Cheng, X., and Guo, L.J., 2004, "A Combined-nanoimprint-and-photolithography Patterning Technique," Microelectronic Engineering, 71(3-4), pp. 277-282.

[7] Zheng, Y., Nguyen, J., Wei, Y., and Sun, Y., 2013, "Recent Advances in Microfluidic Techniques for Single-cell Biophysical Characterization," Lab on a Chip, 13(13), pp. 2464-2483.

[8] Tsai, C.H.D., Tanaka, J., Kaneko, M., Horade, M., Ito, H., Taniguchi, T., Ohtani, T., and Sakata, Y., 2016, "An On-Chip RBC Deformability Checker Significantly Improves Velocity-Deformation Correlation," Micromachines, 7(10), 176, pp. 1-13.

[9] Zheng, Y., Shojaei-Baghini, E., Azad, A., Wang, C., and Sun, Y., 2012, "High-throughput Biophysical Measurement of Human Red Blood Cells," Lab on a Chip, 12(14), pp. 2560-2567.

[10] Hashimoto, S., Mizoi, A., Hino, H., Noda, K., Kitagawa, K., and Yasuda, T., 2014, "Behavior of Cell Passing through Micro Slit," Proc. 18th World Multi-Conference on Systemics Cybernetics and Informatics, 2, pp. 126-131.

[11] Takahashi, Y., Hashimoto, S., Hino, H., and Azuma, T., 2016, "Design of Slit between Micro Cylindrical Pillars for Cell Sorting," Journal of Systemics, Cybernetics and Informatics, 14(6), pp. 8-14.

[12] Jay, A.W.L., 1973, "Viscoelastic Properties of the Human Red Blood Cell Membrane: I. Deformation, Volume Loss, and Rupture of Red Cells in Micropipettes," Biophysical Journal, 13(11), pp. 1166-1182.

[13] Deplaine, G., Safeukui, I., Jeddi, F., Lacoste, F., Brousse, V., Perrot, S., Biligui, S., Guillotte, M., Guitton, C., Dokmak, S., Aussilhou, B., Sauvanet, A., Hatem, D.C., Paye, F., Thellier, M., Mazier, D., Milon, G., Mohandas, N., Mercereau-Puijalon, O., David, P.H., and Buffet, P.A., 2011, "The Sensing of Poorly Deformable Red Blood Cells by the Human Spleen Can be Mimicked In Vitro," Blood, 117(8,) pp. e88-e95.

[14] Hashimoto, S., Otani, H., Imamura, H., et al., 2005, "Effect of Aging on Deformability of Erythrocytes in Shear Flow," Journal of Systemics Cybernetics and Informatics, 3(1), pp. 90-93.

[15] Hashimoto, S., Takahashi, Y., Nakano, Y., Hasegawa, D., Takiguchi, Y., and Yasuda, T., 2018, "Observation of Cell Passing through Single Micro Slit between Weir-walls," Proc. 22nd World Multi-Conference on Systemics Cybernetics and Informatics, 2, pp. 43-48.